



HAL
open science

Hereditary Character of Photonics Structure in Pachyrhynchus sarcitis Weevils: Color Changes via One Generation Hybridization

Yin Chang, Yu Ogawa, Gianni Jacucci, Olimpia D Onelli, Hui-Yun Tseng,
Silvia Vignolini

► **To cite this version:**

Yin Chang, Yu Ogawa, Gianni Jacucci, Olimpia D Onelli, Hui-Yun Tseng, et al.. Hereditary Character of Photonics Structure in Pachyrhynchus sarcitis Weevils: Color Changes via One Generation Hybridization. *Advanced Optical Materials*, 2020, 8, 10.1002/adom.202000432 . hal-03005684

HAL Id: hal-03005684

<https://hal.science/hal-03005684>

Submitted on 25 Nov 2020

HAL is a multi-disciplinary open access archive for the deposit and dissemination of scientific research documents, whether they are published or not. The documents may come from teaching and research institutions in France or abroad, or from public or private research centers.

L'archive ouverte pluridisciplinaire **HAL**, est destinée au dépôt et à la diffusion de documents scientifiques de niveau recherche, publiés ou non, émanant des établissements d'enseignement et de recherche français ou étrangers, des laboratoires publics ou privés.

Hereditary Character of Photonics Structure in *Pachyrhynchus sarcitis* Weevils: Color Changes via One Generation Hybridization

Yin Chang, Yu Ogawa, Gianni Jacucci, Olimpia D. Onelli, Hui-Yun Tseng,* and Silvia Vignolini*

Pachyrhynchus sarcitis weevils are flightless weevils characterized by colored patches of scales on their dark elytra. The vivid colors of such patches result from the reflection of differently oriented 3D photonic crystals within their scales. The results show that hybrid *P. sarcitis*, the first filial generation of two *P. sarcitis* populations from Lanyu Island (Taiwan) and Babuyan Island (Philippines), mixes the color of its ancestors by tuning the photonic structure in its scales. A careful spectroscopical and anatomical analysis of the weevils in the phylogeny reveals the hereditary characteristics of the photonic crystals within their scales in terms of lattice constant, orientation and domain size. Monitoring how structural coloration is inherited by offspring highlights the versatility of photonic structures to completely redesign the optical response of living organisms. Such finding sheds light onto the evolution and development mechanisms of structural coloration in *Pachyrhynchus* weevils and provides inspiration for the design of visual appearance in artificial photonic materials.

colorations with various mechanisms and for diverse functions.^[3,6,16–19] Within the wide variety of architectures and materials exploited by different organisms, insects produce exquisitely complex 3D photonic architectures.^[17,20–22] In the Curculionidae weevil family, most of the species have 3D diamond photonic crystal structures^[22–28] and many species exploit diamond photonic crystals with different volume fractions^[22,23] and lattice constants^[22,23,28] to obtain a wide variety of colorations.

Pachyrhynchus weevils possess a dark exoskeleton marked with colorful patterns. As they are flightless, they are distributed exclusively on several islets of Southeast Asia, and display high insular species diversity.^[29,30] So far, their taxonomy is based only on their optical

appearance^[31–33] and this poor understanding of their ecology often leads to species misidentification.^[34] Moreover, some pioneering works reported incorrect crystal structures^[35,36] and only recent studies^[20,22,27] correctly analyzed the morphology and the optical response of the weevils' scales.

While the optical properties of *Pachyrhynchus* weevils are well characterized and already fascinated several groups in the field, the understanding on how the structural color phenotype is inherited by hybrid weevils, and more in general for insects, is still missing, as it is challenging to grow these species in captivity.^[37]

In this work, we optically and anatomically monitor the evolution of the diamond photonic structure of *P. sarcitis* via a hybridization technique. In particular, we observe that, irrespectively of the sex of the parents, the first-generation cross between captive-bred blue-spotted (Lanyu Is., Taiwan) and yellow-spotted *P. sarcitis* weevils (Babuyan Is., Philippines) inherits a green structural coloration. Such green coloration is not the result of a diamond structure with intermediate lattice constant or chitin filling fraction of the parent weevils, but is related to the orientations and size of the different crystal domains within their scales.

By combining the statistical information on the morphology of the crystal, domain sizes, and orientations (obtained by multi-directional scanning electron microscope (SEM) images) with the numerical calculation, we reproduce the measured optical response. Our results reveal the significance of the preferred domain orientations on the visual

1. Introduction

Structural colors, i.e., colors originating from interactions of light and nanostructured materials, are incredibly widespread in living organisms.^[1–3] From bacteria,^[4] to plants,^[5,6] insects,^[7–13] and larger animals.^[14–16] Different organisms produce bright

Y. Chang, G. Jacucci, Dr. O. D. Onelli, Dr. S. Vignolini
Department of Chemistry
University of Cambridge
Cambridge CB2 1EW, UK
E-mail: sv319@cam.ac.uk

Dr. Y. Ogawa
Univ. Grenoble Alpes
CNRS
CERMAV
Grenoble 38000, France

Dr. H.-Y. Tseng
Department of Entomology
National Taiwan University
Taipei City 106, Taiwan
E-mail: hytseng1216@ntu.edu.tw

 The ORCID identification number(s) for the author(s) of this article can be found under <https://doi.org/10.1002/adom.202000432>.

© 2020 The Authors. Published by WILEY-VCH Verlag GmbH & Co. KGaA, Weinheim. This is an open access article under the terms of the Creative Commons Attribution License, which permits use, distribution and reproduction in any medium, provided the original work is properly cited.

DOI: 10.1002/adom.202000432

appearance of the weevil scales, providing important insights on the factors shaping the evolution of structural colors in weevils. In fact, the tuning of the distribution of the domain orientations might be a convenient strategy to achieve different colorations, strengthening the hypothesis of the self-assembly characteristics of the morphogenesis of photonic structures in insects via phase separation processes.^[7,17,21] Finally, we discuss how these findings might provide a convenient strategy to optimize visual appearance with structurally colored materials.

2. Results

2.1. Optical Appearance and Reflection Spectra of Weevils' Scales

All three *P. sarcitis* weevils exhibit patterns of colored patches of scales in similar locations on their dark exoskeletons (Figure 1). Macroscopically, the Lanyu *P. sarcitis* (LPS) has blue and cyan scales (Figure 1A), Babuyan *P. sarcitis* (BPS) has predominantly

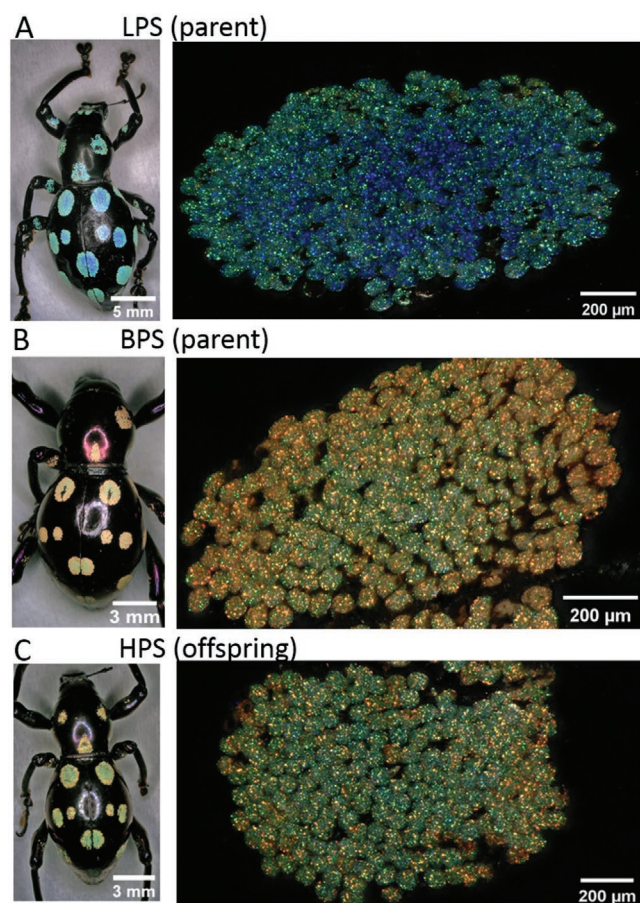


Figure 1. Three *Pachyrhynchus sarcitis* (*P. sarcitis*) used in this study and the enlarged image of a single pit of each weevil. A) Lanyu *P. sarcitis* (LPS, from Lanyu Is., Taiwan) and B) Babuyan *P. sarcitis* (BPS, from Babuyan Is., Philippines) are captive species. C) Hybrid *P. sarcitis* (HPS) is the filial generation of LPS and BPS. For all three weevils each pit is covered by many small scales.

green and yellow scales (Figure 1B), while their offspring, hybrid *P. sarcitis* (HPS), has green scales (Figure 1C).

In the epi-illumination microscope pictures reported in Figure 2A–C, we can observe that for all three weevils every scale shows differently colored areas (domains) with colors in the entire visible spectral range. Therefore, in order to quantitatively correlate how such domains cumulatively contribute to the overall optical appearance, we measured: i) the reflection spectrum of each single domain in several areas for all three weevils (in terms of spectral position and intensity), ii) their lateral size, and iii) their abundance. Representative spectra are reported in Figure 2D–F, while all spectra, images, domain color histograms, and their statistic domain color coverage for the examined scales are provided in Figures S1 and S2 and Table S1 (Supporting Information).

As reported in Figure 2, for all three weevils it is possible to find domains reflecting colors across the entire visible spectral range from blue to red, with a full width at half maximum (FWHM) of ranging from 30 to 108 nm, with generally, a larger FWHM for red-shifted peaks. Interestingly, we notice that the intensity of the reflection peaks varies in different weevils depending on the spectral region: as an example, cyan and green are the most intensely reflected colors in LPS. While, in

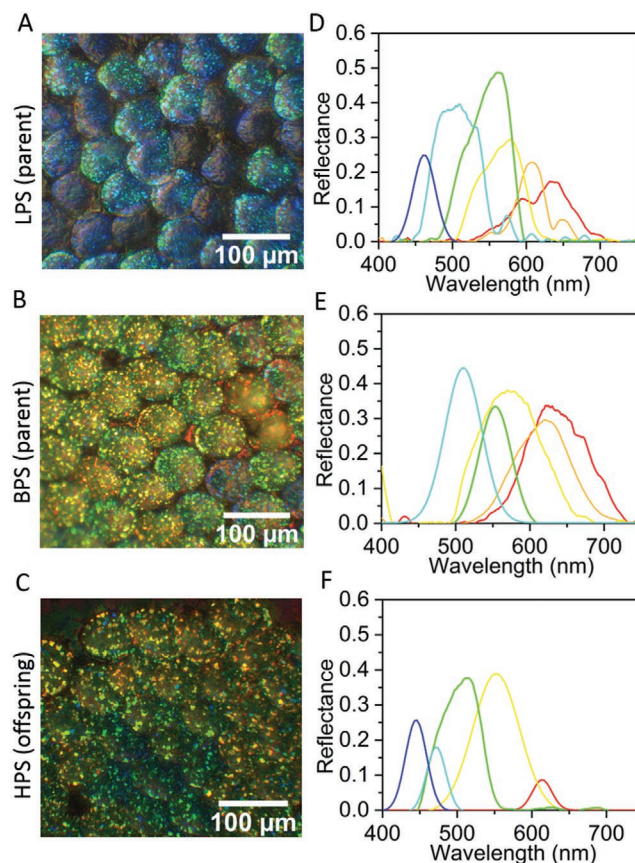


Figure 2. Differently colored domains within the scales and representative reflected spectra of each domain color in the three weevils. A–C) Domains with different colors can be recognized in each scale of all three weevils. Blue, yellow, and green are dominant color in LPS, BPS, and HPS, respectively. D–F) The representative spectra for LPS, BPS, and HPS originating from differently colored domains in the scales.

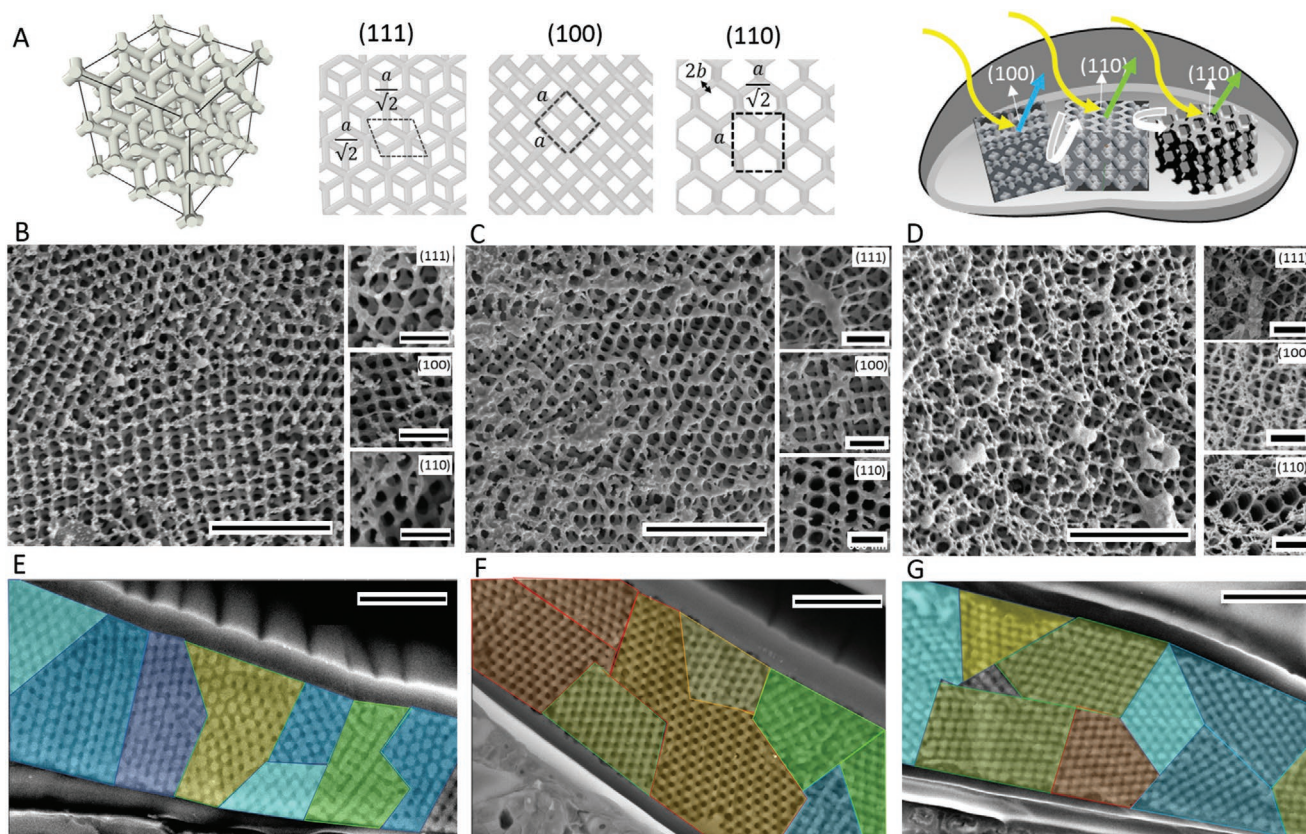


Figure 3. Three-dimensional photonic crystals with single diamond lattice structure (Fd-3m) in three weevils and mapping domain orientations and reflected color normal to the scale surfaces. A) Illustrations of a single diamond lattice and its three characteristic orientations: (111), (100), (110). Lattice constant, a , can be calculated from the three characteristic orientations. B–G) Different oriented domains (rotating horizontally (azimuth angle φ) or tilting (polar angle θ) from crystal normal [100]) are observed in both top view and cross-section SEM images in (B,E) LPS, (C,F) BPS, and (D,G) HPS, confirming that different color domains correspond to different crystal orientations for the three weevils. Scale bars in (B–G) are 2 μm , while in (111), (100), (110) images are 500 nm. It is possible to observe in the three weevils that, at the side of one scale, the top and base of the shell are connected by one domain as shown in (E) LPS, or by two domains as shown in (F) BPS and (G) HPS.

BPS, all the reflected colors have a comparable reflectance, and the HPS exhibits a higher reflectance of green and yellow.

2.2. Domain Orientations and Lattice Parameters

To quantify the size and occurrence of the domains, we imaged the photonic crystal structures inside the scales via SEM both from above and in cross-section (see **Figure 3**); detailed sample preparation is described in the Experimental Section. Multiple crystal orientations were observed from both top views (Figure 3B–D) and cross-sectional views (Figure 3E–G), indicating that crystals rotate in three dimensions in all three weevils. The typical patterns of the diamond crystal orientations (100), (110), (111) have been observed in all three weevils (Figure 3A–D). From SEM images of (111), we estimated the lattice constant, a , while we measured the strut radius, b , from cross-sectional SEM images of (110) orientation, as, in this direction, the strut is perpendicular to the observation plane. The air pore radius, R , is then calculated from the measured strut radius and lattice constant with the diamond lattice structure relation: $R = a/2 - \sqrt{2}b$, see also Figure S3 and Table S2 in the Supporting Information for additional details.

Quantitative structural information was obtained by sampling over a large number of regions within scales and between scales from different areas of the weevils' exoskeleton. The average strut radius, lattice constant, pore radius and filling fraction (FF of diamond minimum surface model) for the three weevils are shown in **Table 1**. It is interesting to highlight that all three weevils have similar strut radii of 57–59 nm and FF of 0.4. In contrast, the LPS weevil has a lattice constant of $a = 413 \pm 5$ nm, while BPS and HPS have similar values for the lattice constant ($a = 439 \pm 7$ nm and $a = 444 \pm 5$ nm, respectively).

Table 1. Measured strut radius and lattice constant from SEM images, and the calculated pore radius and filling fraction of the three weevils.

	LPS (parent)	BPS (parent)	HPS (offspring)
Strut radius, r (nm)	58.5 ± 6.5	57.4 ± 5.9	59.4 ± 6.2
Lattice constant, a (nm)	412.8 ± 5.4	438.5 ± 6.7	443.9 ± 5.4
Pore radius (calculated)	123.7 ± 9.6	138.1 ± 9.0	137.9 ± 9.2
Pore/ a	0.3 ± 0.1	0.3 ± 0.1	0.3 ± 0.1
Filling fraction, FF (Diamond Minimum Surface)	0.4 ± 0.1	0.4 ± 0.1	0.4 ± 0.1

From the cross-sectional SEM images, we also estimate the domain sizes at the base and top of the scale, see Table S2 in the Supporting Information. In general, we observe that all three weevils have scales thickness of 2–3 μm . In LPS, most domains range between 1.5 to 2.5 μm in width (65 of the 67 domains investigated). In BPS, the width of the domain ranges between 2.5 and 3.5 μm (77 out of 79 domains investigated), while HPS has more varied domain widths that range from 1.5 to 3.5 μm (60 domains observed). Additionally, we observe that: i) LPS has a smaller average domain size than BPS and HPS, and possesses many domains connecting both the top and the base of the scale; ii) at the edges of the scale, domains that connect the top and the base of the scale can be observed while this is not the case at the center of the scale.

2.3. FDTD Simulation and Visual Color Appearance

To correlate the orientation of the domains with the macroscopic optical response, we compute FDTD reflection spectra for the most abundant domains in each weevil, using the measured domain sizes, see Figure S4A–C (Supporting Information). The calculated spectra considering the effects of the domain width, domain thickness, the boundary conditions and presence of disorder are provided in Figure S5 (Supporting Information), and a complete discussion on how these parameters affect the optical response is also reported in the Supporting Information. This characterization allows us to assign each reflected color to a specific domain orientation identified via SEM. By comparing the histogram of colors obtained by RGB image analysis in Figure 4A,D,G (see the Experimental Section) with the histogram of the domain orientations multiplied by the average lateral size of the domains in Figure 4B,E,H, we show that the macroscopic color of each weevil is the sum of the contribution of individual domains, and that the distribution of orientations is the determining factor in the different color appearances of the three weevils. To facilitate the reader to visualize the correlation between the orientation of the domains with the macroscopic optical response, we plot the area covered by each oriented domain in the three weevils on a stereographic projection in Figure 4C,F,I (as the insets of Figure 4 in ref. [40]).

In the projections, each marker corresponds to a specific domain orientation of the photonic structure inside the scale. The size of the markers is proportional to the area covered by the domain, and the color of the markers is chosen accordingly to the reflected color by the domains.

If we define a spherical coordinate system where the normal of crystal plane (100) as the zenith direction, (with φ defining the azimuthal angle, and θ defining the polar angle, see Figure 3A and Figure S7, Supporting Information), we observe different features of the angular relationships of preferred domain orientations in three weevils. The preferred domains orientations in LPS are along $\varphi = 0^\circ$ – 45° . In BPS, most of the domains are along $\varphi = 45^\circ$ and 26.6° for which the reflected colors are red-shifted and domain coverage decreases from $\varphi = 26.6^\circ$ to 0° . Preferred domain orientations in HPS are comparatively more evenly distributed (see also the Supporting Information “Domain orientations and domain color distributions” section,

Figure S4D–F and Table S3 in the Supporting Information for detail discussion).

We believe that the color-changing strategy of the hybrid weevil is interesting to design appearance with photonic materials because it relies on two main features that have high, but currently underexploited, potential: the combined use of an asymmetrical hierarchical structure and the optimization of size and distribution of domain with different orientation.

First, the photonic structure is confined into an asymmetrical scale that has a lateral size much larger than the thickness. Such a hierarchical feature allows minimizing the amount of material necessary to produce the desired coloration. In contrast, artificial hierarchical photonic structures propose so far usually consist of spherical structures,^[41] where a significant fraction of the photonic crystal does not contribute to the optical response.

Second, the ability of the HPS to fine-tune color by optimization of domain size and distribution or the photonic crystal orientation, without a change of lattice constant. Such strategy is general and can be extended not only to bi-continuous types of photonic crystals but to any 3D and 2D ones. In contrast, the most used approach up to now to tune coloration in artificially photonic crystals systems is to change the lattice constant: requiring a change of the building blocks composing the photonic crystals, (nanosphere size in case of opal-like structures made by colloidal self-assembly or polymer chain length in case of other photonic crystals made of block-copolymers).^[41–43]

3. Conclusion

The possibility to captive-breed and hybridize different structurally colored *Pachyrhynchus* weevils allowed us to systematically investigate how photonic structures can be modified from ancestors to descendent only in one generation. By carefully studying the anatomy of the scales of the three weevils, we observed that the captive-bred hybrid *P. sarcitis* obtain green coloration by maintaining the lattice constant of its ancestors (BPS) and changing the domain size and orientations.

Interestingly, these observations remain valid irrespectively of the sex of the parents. Hybrid *P. sarcitis* weevils from blue and yellow parents are always green. To gather a full understanding of the heredity characters of this system will require genetic mapping of all animals. However, if we define the lattice constant of the photonic structure as a phenotypic trait, we can hypothesize that the genes of the BPS ancestor are dominant. By looking at the sequences of the different weevils, one would therefore expect to find similarities between the offspring and one parent generation, while similar occurrences are not expected to be found with the other parent. Additionally, if we consider the domain orientation as a possible phenotypic trait, we can conclude that the genetic variation in HPS seems to be additive as the domain orientation is about the average of those of the parents.

We speculate that changing orientation of domains to tune color might be more successful than an adjustment of the lattice constant if one consider that such nanostructures are obtained via self-assembly of an infolding lipid-bilayer membrane, followed by deposition of chitin into the extra-cellular space.^[7,17,21] In this hypothesis a change of lattice constant will,

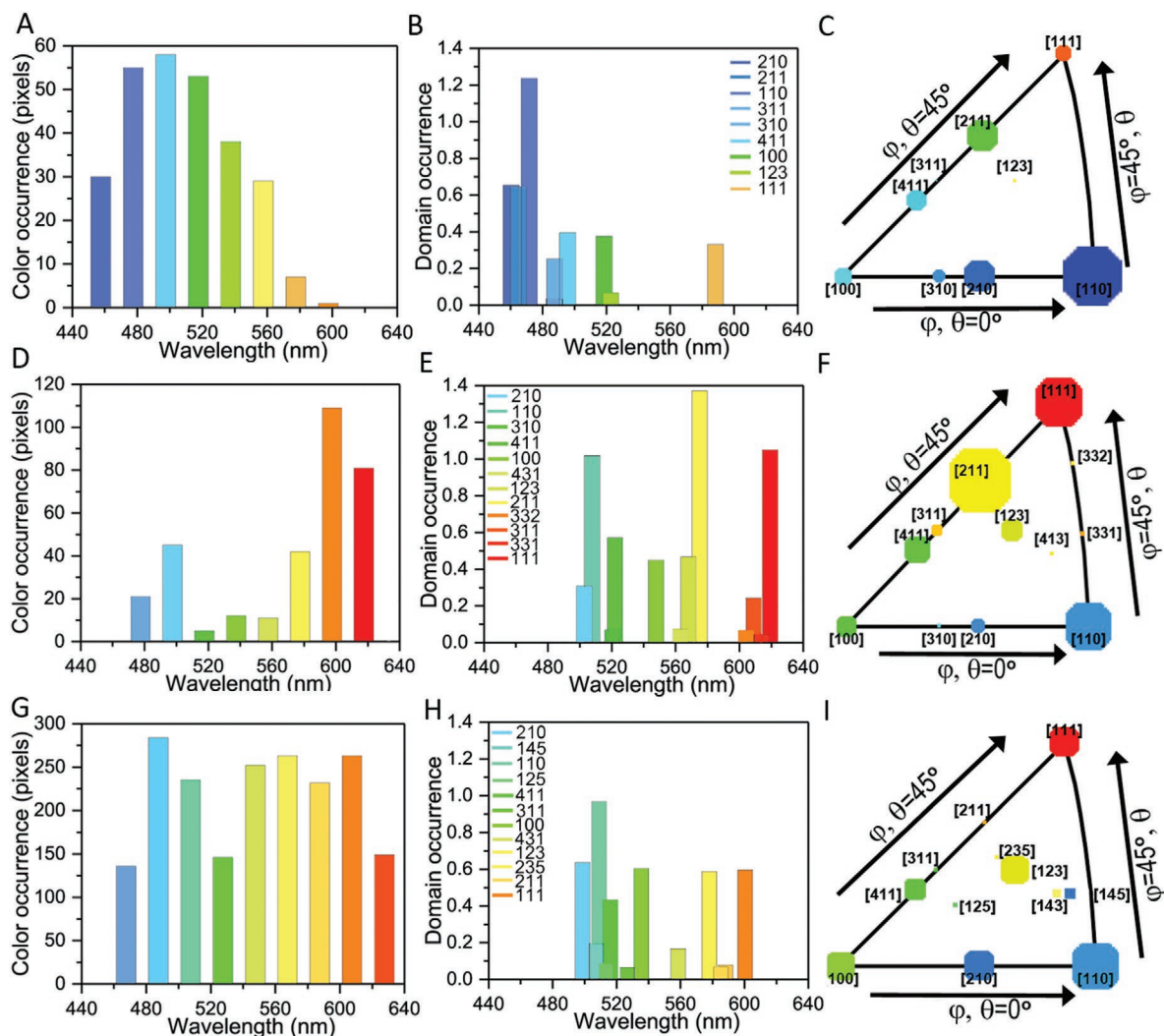


Figure 4. Comparison of color of color derived by RGB image analysis on optical microscope images and domain occurrence derived by statistical analysis on SEM images of A–C) LPS, D–F) BPS, G–I) HPS. In (A,D,G) we show the distribution of color on the scales of three weevils. The color histograms are obtained using image analysis on individual scales and then averaging. In (B,E,H) we report the histogram of the area covered by each domain orientation for three weevils. The domain occurrence is obtained by multiplying the number of a domain with its average width and normalized on the average radius of the scale which is $38.08 \pm 1.1 \mu\text{m}$ for LPS; $36.42 \pm 0.5 \mu\text{m}$ for BPS, and $37.10 \pm 6.3 \mu\text{m}$ for HPS. In (C,F,I) we illustrate the preferred domain orientations in three weevils on stereographic projection with the marker size proportional to the domain occurrence and the marker color the same as the reflected color.

in fact, require a re-design of the biopolymers involved in the formation of these photonic structures, while changes in crystal domain orientations can be simply achieved by a change in surface properties in the scale interior membrane.

Moreover, a fast adaptation mechanism that can be obtained in one generation only might be of advantage under selection pressures from predation. This is further confirmed by the fact that the colored patches of *Pachyrhynchus* weevils are known to have aposematic functions^[19,30] as their robust exoskeleton form a co-defense mechanism that efficiently reduces attack rate from local lizards.^[19] In fact, several different genera of weevils^[29,31] such as long-horned beetles (*Doliops* spp.) and crickets (*Scopastus pachyrhynchoides*)^[29,31,38] occurring in the same geographical area display a similar bright pattern of colors. Finally, the possibility to study the hereditary character of structural colors in

captive-bred species also allows, in future studies, to gain a better understanding of the development of such nanostructures.

By quantitatively correlating the measured optical response and anatomy of the hybrid *P. sarcitis* with the ones of its ancestors, we reveal how structural colors in *Pachyrhynchus* can be readily tuned in only one generation by adjusting the orientations of the photonic crystal domains in its scales. Monitoring how the structural colors traits can be passed to the first filial generation we speculate that poly-domains 3D photonic structures may represent a successful strategy for changing appearance in presence of strong selection pressure. Our result that the hybrid weevils have domain tilting and no change of the lattice constant provides an interesting inspiration for visual appearance design using self-assembly techniques for photonic materials.^[41,43]

4. Experimental Section

Species Selections: Adults of *P. sarcitis* were collected from Babuyan (19°32' 58"N, 121°54' 40"E) and Lanyu (22°4'44.57"N, 121°33'15.25"E) Islands. These two populations have almost identical appearances, except coloration. Captive-breeding of Lanyu *P. sarcitis*, Babuyan *P. sarcitis* and hybrid *P. sarcitis* were conducted in the laboratory in National Taiwan University (Taipei, Taiwan). The detail of the breeding technique can be found in the paper.^[37]

Optical Microscopy and Image Analysis: Optical microscopy was performed using a Zeiss Axio Scope optical microscope in Köhler illumination equipped with a 50X SLWD objective (Nikon, NA = 0.4) coupled to a spectrometer (Avantes HS2048) via an optical fiber (Thorlabs, FC-UV100-2-SR) (detected spot with diameter of a few μm). Spectra were normalized with a silver mirror (Thorlabs, PF10-03-P01). Scales were detached from the elytra and placed on glass slide. Spectra of different domains on each scale were measured. Domain color distribution was quantitatively analyzed by image-based RGB analysis on many single scales in each weevil with ImageJ Software (<http://rsb.info.nih.gov/ij/>).^[39]

SEM Sample Preparation and Image Analysis: For the top view SEM images, scales were detached from the elytra and placed on a glass slide and plasma etched for 13 min to remove the outer shell of scales. The etched scales were transferred onto a SEM Stub and coated with 10 nm Pt for imaging. The SEM (TESCAN MIRA3 FEG-SEM) used to observe the top view was operated at 3 kV with working distance of 5.2 mm and using an in-beam secondary electron detector.

For the cross-sectional imaging, the scales still attached to the elytra were directly embedded in Embed 812 resin (EMS, Hatfield, USA) and hardened overnight at 60 °C. After resin embedding, the scales were transversely cut (with a 35° diamond knife (Diatom, USA) equipped on a ultramicrotome Leica EM UC6 (Leica Microsystems, Germany) to expose their internal voids on the block face. Fresh resin was then applied again on the block face to fill the inside of the scale. Once the resin set scales were cut again using the same setup. The newly made block face was further treated with 2% osmium tetroxide aqueous solution to enhance image contrast. The cross-sectional SEM observation was carried out with a field emission SEM (Quanta-FEG 250, Thermo Fisher Scientific Inc., USA) operated at 7 kV and using a concentric backscattering electron detector.

FDTD Simulation: Three dimensional diamond models were constructed in MATLAB and 3D images were obtained with Blender. Finite-difference time-domain (FDTD) calculations were performed with the commercial software Lumerical. Different crystal orientations, characterized through cross-sectional SEM images of scales, were oriented in the simulation box perpendicular to the direction of light incidence. Reflection properties of the chitin-air diamond structures were modelled with experimentally determined refractive index $n = 1.53$ for chitin (measured via index matching oils Cargille series A), and $n = 1$ for the air spaces. Diamond minimum surface equation $f(X, Y, Z) = \cos(Z) \sin(X + Y) + \sin(Z) \cos(X - Y)$ ^[9] was used for model construction, where $X = 2\pi x/a$, $Y = 2\pi y/a$, $Z = 2\pi z/a$ with a the lattice constant, and x , y , and z the coordinates. To match the experimental measurement conditions, the simulation models were constructed with measured domain sizes, boundary conditions were set to perfectly matched-layer boundaries (PML) in x , y , and z , and light source was set to Gaussian distributed from 300–800 nm with numerical aperture (NA) = 0.4. One simulation run of these setups for one orientation in one weevil required a memory of ≈ 30 –60 GB and simulation time 6–10 ns for 20–36 calculation hours. The solution of domains with bigger size require longer simulation time to converge. The FDTD results were compared with different boundary conditions: PML with different domain sizes and periodic boundary conditions (Figure S5, Supporting Information). FWHM and reflectance were also calculated considering effect of numerical aperture and disorder. To correlate the color with the different orientations in the three weevils, the simulation boundary conditions were set to be periodical for x and y dimensions. The z direction was set to be PML to take into account the measured limited thickness. This setting enables to simulate a much smaller model in x , y dimension by constructing a minimum repeated unit cell, so to save computation resources that for one simulation run

required a memory of ≈ 0.5 –0.8 GB, and shorter simulation time of 3 ns for deriving convergent solutions in 0.5–1.5 calculation hours. Even though in this setup, the precision was lost in domain width and a plane wave light source (NA = 0) was assumed.

Supporting Information

Supporting Information is available from the Wiley Online Library or from the author.

Acknowledgements

The authors thank Hsin-Chieh Tang and Lung-Chun Huang (Taipei Zoo, Taiwan) and Wen-San Huang (National Museum of Natural Science, Taiwan) for the captive-breeding technique support of weevils. The authors also appreciate the endangered species research numbers (Nos. 1061701832 and 1080231159) issued by the Council of Agriculture, Taiwan. Y.O. thanks NanoBio-ICMG platform (FR 2607) for granting access to the electron microscopy facility. This work was supported by the Cambridge Trust, the BBSRC David Phillips fellowship [BB/K014617/1] and the ERC SeSaME ERC-2014-STG H2020 639088. Photography credits go to Lung-Chun Huang (Taipei Zoo, Taiwan)

Conflict of Interest

The authors declare no conflict of interest.

Author Contributions

Y.C., O.D.O., H.Y.T., and S.V. designed research; H.Y.T. captive-bred and hybridized Pachyrhynchus weevils; Y.C., Y.O., and O.D.O. processed SEM data; Y.O. embedded, fixed and microtomed the samples for SEM imaging. Y.C., O.D.O. measured domain spectra; Y.C., O.D.O., and S.V. performed and analyzed optical/SEM data; Y.C. and O.D.O. conducted MPB and FDTD simulation; G.J. conducted semi-analytical analysis for disorder; Y.C. and H.Y.T. organized crystal structures of Entiminae subfamily and H.Y.T. analyzed the data for discussing biofunctions of structural color and phylogeny of Pachyrhynchus weevils; Y.C., Y.O., O.D.O., G.J., H.Y.T., and S.V. discussed results and commented on the manuscript. Y.C., H.Y.T., and S.V. wrote the paper.

Keywords

hereditary structural colors, hybridization, *Pachyrhynchus* weevils, preferred orientations, self-assembly

Received: March 12, 2020

Revised: April 14, 2020

Published online: May 14, 2020

- [1] S. Kinoshita, *Structural Colors in the Realm of Nature*, World Scientific, Singapore 2008.
- [2] S. Vignolini, N. Bruns, *Adv. Mater.* **2018**, *30*, 1801687.
- [3] V. E. Johansen, O. D. Onelli, L. M. Steiner, S. Vignolini, in *Photonics in Nature: From Order to Disorder*, Springer International Publishing, Cham 2017, pp. 53–89.
- [4] V. E. Johansen, L. Catón, R. Hamidjaja, E. Oosterink, B. D. Wilts, T. S. Rasmussen, M. M. Sherlock, C. J. Ingham, S. Vignolini, *Proc. Natl. Acad. Sci. USA* **2018**, *115*, 2652.

- [5] S. Vignolini, P. J. Rudall, A. V. Rowland, A. Reed, E. Mourold, R. B. Faden, J. J. Baumberg, B. J. Glover, U. Steiner, *Proc. Natl. Acad. Sci. USA* **2012**, *109*, 15712.
- [6] K. R. Thomas, M. Kolle, H. M. Whitney, B. J. Glover, U. Steiner, *J. R. Soc., Interface* **2010**, *7*, 1699.
- [7] H. Ghiradella, *J. Morphol.* **1989**, *202*, 69.
- [8] R. W. Corkery, E. C. Tyrode, *Interface Focus* **2017**, *7*, 20160154.
- [9] K. Michielsen, D. G. Stavenga, *J. R. Soc., Interface* **2008**, *5*, 85.
- [10] M. E. McNamara, V. Saranathan, E. R. Locatelli, H. Noh, D. E. G. Briggs, P. J. Orr, H. Cao, *J. R. Soc., Interface* **2014**, *11*, 20140736.
- [11] R. Ebihara, H. Hashimoto, J. Kano, T. Fujii, S. Yoshioka, *J. R. Soc., Interface* **2018**, *15*, 20180360.
- [12] M. H. Bartl, J. W. Galusha, L. R. Richey, J. S. Gardner, J. N. Cha, *Phys. Rev. E* **2008**, *77*, 050904.
- [13] D. V. Nance, *Interim Rep.* **2013**, <https://doi.org/10.21236/ada570980>.
- [14] M. Srinivasarao, *Chem. Rev.* **1999**, *99*, 1935.
- [15] H. Yin, B. Dong, X. Liu, T. Zhan, L. Shi, J. Zi, E. Yablonovitch, *Proc. Natl. Acad. Sci. USA* **2012**, *109*, 10798.
- [16] R. O. Prum, R. H. Torres, *J. Exp. Biol.* **2004**, *207*, 2409.
- [17] V. Saranathan, C. O. Osuji, S. G. J. Mochrie, H. Noh, S. Narayanan, A. Sandy, E. R. Dufresne, R. O. Prum, *Proc. Natl. Acad. Sci. USA* **2010**, *107*, 11676.
- [18] J. A. Endler, *Philos. Trans. R. Soc., B* **1993**, *340*, 215.
- [19] H. Y. Tseng, C. P. Lin, J. Y. Hsu, D. A. Pike, W. S. Huang, *PLoS One* **2014**, *9*, 91777.
- [20] A. E. Seago, P. Brady, J. P. Vigneron, T. D. Schultz, *J. R. Soc., Interface* **2009**, *6*, S165.
- [21] B. D. Wilts, B. A. Zubiri, M. A. Klatt, B. Butz, M. G. Fischer, S. T. Kelly, E. Spiecker, U. Steiner, G. E. Schröder-Turk, *Sci. Adv.* **2017**, *3*, 1603119.
- [22] B. D. Wilts, V. Saranathan, *Small* **2018**, *14*, 1870212.
- [23] J. W. Galusha, L. R. Richey, M. R. Jorgensen, J. S. Gardner, M. H. Bartl, *J. Mater. Chem.* **2010**, *20*, 1277.
- [24] A. E. Seago, R. Oberprieler, V. K. Saranathan, *Integr. Comp. Biol.* **2019**, *59*, 1664.
- [25] B. D. Wilts, K. Michielsen, H. DeRaedt, D. G. Stavenga, *J. R. Soc., Interface* **2012**, *9*, 1609.
- [26] B. D. Wilts, K. Michielsen, J. Kuipers, H. De Raedt, D. G. Stavenga, *Proc. R. Soc. B* **2012**, *279*, 2524.
- [27] V. Saranathan, A. E. Seago, A. Sandy, S. Narayanan, S. G. J. Mochrie, E. R. Dufresne, H. Cao, C. O. Osuji, R. O. Prum, *Nano Lett.* **2015**, *15*, 3735.
- [28] R. K. Nagi, D. E. Montanari, M. H. Bartl, *Bioinspiration Biomimetics* **2018**, *13*, 035003.
- [29] W. Schultze, *Philipp. J. Sci.* **1923**, *23*, 609.
- [30] C. Y. Lee, S. P. Yo, R. W. Clark, J. Y. Hsu, C. P. Liao, H. Y. Tseng, W. S. Huang, *J. Zool.* **2018**, *306*, 36.
- [31] Y. Hiraku, *Gekkan-Mushi* **2017**, *553*, 22.
- [32] A. Rukmane, *Acta Biol. Univ. Daugavpiliensis* **2017**, *17*, 85.
- [33] Y. T. Chen, H. Y. Tseng, M. L. Jeng, Y. C. Su, W. S. Huang, C. P. Lin, *Systematic Entomology* **2017**, *42*, 796.
- [34] A. R. Parker, V. L. Welch, D. Driver, N. Martini, *Nature* **2003**, *426*, 786.
- [35] V. Welch, V. Lousse, O. Deparis, A. Parker, J. P. Vigneron, *Phys. Rev. E* **2007**, *75*, 041919.
- [36] V. L. Welch, J. P. Vigneron, *Opt. Quantum Electron.* **2007**, *39*, 295.
- [37] L. C. Huang, W. S. Huang, C. P. Lin, O. M. Nuñez, H. Y. Tseng, H. C. Tang, *J. Asia-Pac. Entomol.* **2018**, *21*, 1233.
- [38] A. Barševskis, N. Savenkov, *Balt. J. Coleopterol.* **2013**, *13*, 91.
- [39] J. Schindelin, I. Arganda-Carreras, E. Frise, V. Kaynig, M. Longair, T. Pietzsch, S. Preibisch, C. Rueden, S. Saalfeld, B. Schmid, J.-Y. Tinevez, D. J. White, V. Hartenstein, K. Eliceiri, P. Tomancak, A. Cardona, *Nat. Methods* **2012**, *9*, 676.
- [40] B. Winter, B. Butz, C. Dieker, G. E. Schröder-Turk, K. Mecke, E. Spiecker, *Proc. Natl. Acad. Sci. USA* **2015**, *112*, 12911.
- [41] E. S. A. Goerlitzer, R. N. Klupp Taylor, N. Vogel, *Adv. Mater.* **2018**, *30*, 1706654.
- [42] B. D. Wilts, P. L. Clode, N. H. Patel, G. E. Schröder-Turk, *MRS Bull.* **2019**, *44*, 106.
- [43] M. Stefk, S. Guldin, S. Vignolini, U. Wiesner, U. Steiner, *Chem. Soc. Rev.* **2015**, *44*, 5076.